

A Flexible Tri-carboxylic Acid Derived Zinc(II) 3D Helical Metal-Organic-Framework and a Cadmium(II) Interwoven 2D Layered Framework Solid

Pratap Vishnoi^[a] and Ramaswamy Murugavel^{*[a]}

Dedicated to Professor C. N. R. Rao on the Occasion of His 80th Birthday

Keywords: Flexible tri-carboxylate ligand; Helical structures; Metal-organic frameworks; Tetrahedral arrangement; Twofold interpenetration; Layered compounds

Abstract. Starting from a flexible tri-carboxylic acid ligand H_3L ($H_3L = 2,4,6$ -tris[(4'-carboxyphenoxy)methyl]-1,3,5-trimethylbenzene), a 3D metal-organic framework $[Zn(HL)(H_2O)]_n$ (**1**) and a 2D polymeric layered solid $\{[(CH_3)_2NH_2]_2[Cd_2L_2(DMA)_2]\}_n$ (**2**) were hydrothermally synthesized. The complexes were characterized by elemental analyses, FT-IR spectroscopy, TGA, and single-crystal X-ray diffrac-

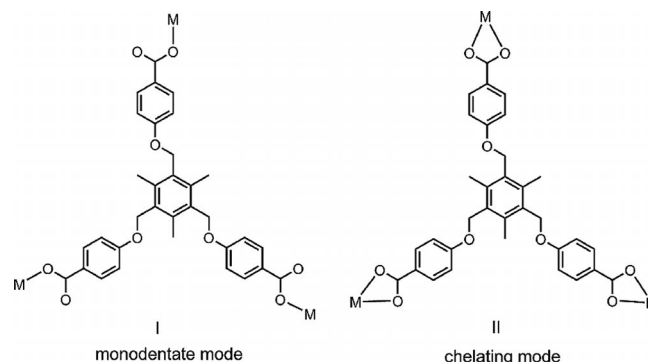
tion. The X-ray structural analyses reveal that the complex **1** is an example of a doubly interpenetrated 3D helical MOF with mutually entwined right- and left-handed helices to form an overall racemic framework. Complex **2** is made up of fourfold interwoven 2D nets in the solid state.

Introduction

In recent years, metal-organic framework (MOF) materials have attracted widespread attention owing to their interesting properties and potential applications as gas storage and separation materials,^[1,2] luminescent sensors,^[3–5] magnetic materials,^[6] and catalysts.^[7] MOFs with helical structure are of particular interest because of their relevance to bio-molecules such as DNA and proteins, which living organisms utilize for coding genetic information.^[8,9]

It is well studied in MOF chemistry that several factors such as metal coordination arrangement, solvent, reaction conditions, and pH etc. contribute to the topology of the desired framework.^[10,11] Therefore, a judicious selection of building units can lead to helical MOFs with specific structures and functions. Towards synthesizing helical MOFs, one of the most contributing factors is the denticity and flexibility of the ligand system(s). The flexible multidentate acid ligands have been known to adopt various conformations and can curve when coordinate with metal ions. In this regard, aromatic multidentate ligands are good connectors and have opportunity to form helical structures.^[13–16] Over past few years, the chemistry of helical structures have been well developed employing flexible C_2 symmetric ligands.^[17–19]

To the best of our knowledge, helical MOFs with C_3 symmetric ligands are rare. In the presented study the synthesis



Scheme 1. Coordination modes of H_3L in complexes **1** and **2**.

and structural characterization of a 3D MOF of Zn^{II} with 1D helical channels, $[Zn(HL)(H_2O)]_n$ (**1**) and a 2D layered MOF of Cd^{II} , $\{[(CH_3)_2NH_2]_2[Cd_2L_2(DMA)_2]\}_n$ (**2**), were achieved. Owing to the flexibility of the ligand, helical features were introduced into **1**, where each carboxylate anion of the ligand exhibits monodentate mode of coordination (Scheme 1). The chelating mode of the carboxylates in **2** produces a 2D structure. While this work has been in progress, other framework structures of H_3L with Zn^{II} and Cd^{II} ions have been reported; these structures have however been obtained using different reaction conditions and co-ligands, exhibiting different molecular topologies.^[20,21]

Results and Discussion

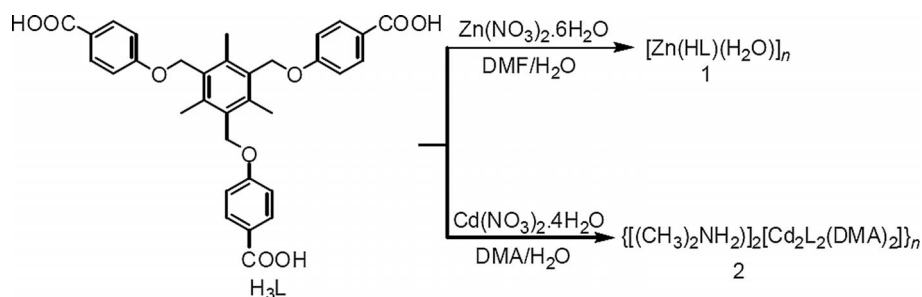
Synthesis

Colorless bulk crystals of $[Zn(HL)(H_2O)]_n$ (**1**) were obtained by hydrothermal treatment of H_3L with $Zn(NO_3)_2 \cdot 6H_2O$

* Prof. Dr. R. Murugavel
Fax: + 91-022-2576-7152
E-Mail: rmv@chem.iitb.ac.in

[a] Department of Chemistry
Indian Institute of Technology Bombay
Mumbai – 400 076, India

Supporting information for this article is available on the WWW under <http://dx.doi.org/10.1002/zaac.201300677> or from the author.



Scheme 2. Synthetic routes for **1** and **2**.

in DMF/H₂O solvent mixture (Scheme 2). However the hydrothermal synthesis involving Cd(NO₃)₂·4H₂O performed in DMF/H₂O solvent mixture yielded only an amorphous powder. The replacement of DMF with DMA resulted in X-ray quality colorless crystals of {[(CH₃)₂NH₂]₂ [Cd₂L₂(DMA)₂] }_n (**2**). Molecular compositions of the complexes were determined by elemental analyses, FT-IR spectroscopy, and single-crystal X-ray diffraction studies.

FT-IR and Thermogravimetric Analysis

The formation of metal carboxylate bonds in **1** and **2** were verified with the aid of FT-IR spectra (Figure S1, Supporting Information). Two intense peaks appearing at around 1600 and around 1390 cm⁻¹ correspond to the antisymmetric and symmetric C=O (carboxylate) stretching vibrations.

Thermogravimetric analyses were performed at heating rate of 10 °C·h⁻¹ from room temperature to 1000 °C under continuous flow of nitrogen gas. Both complexes show similar thermal decomposition behavior and exhibit two weight losses (Figure S2, Supporting Information). A rather continuous weight loss observed up to ca. 250 °C is attributable to the loss of solvent molecules (coordinated/uncoordinated) present in the complexes. After removal of the solvent molecules, gradual decomposition of organic ligands occurs in the temperature range of 330–500 °C.

Crystal Structure Analyses

Crystal Structure of [Zn(HL)(H₂O)]_n (**1**)

A detailed X-ray structure analysis suggests that the complex crystallizes as a 3D helical network in the monoclinic *C2/c* space group. The fundamental structural unit consists of one tetra-coordinated Zn^{II} ion, one doubly deprotonated HL²⁻ ligand, and one terminally coordinated aqua ligand (Figure S3, Supporting Information). Three coordination sites of Zn^{II} ion are occupied by carboxylic oxygen atoms and the fourth one is occupied by an aqua ligand, thus providing a tetrahedral arrangement around the central Zn^{II} ions. In other words, each HL²⁻ ligand binds with three different Zn^{II} ions through monodentate coordination modes, which can be described as (η¹-η¹-η¹)-μ₃ mode of coordination.

The Zn–O(carboxylate) distances fall in the range of 1.947–1.968 Å (Table 1), whereas the Zn–O(water) bonds were found to be slightly longer with bond lengths of 2.009 Å. One of the

Table 1. Selected bond lengths /Å for **1** and **2**.

1			
Zn(1)–O(5)	1.941(3)	Zn(1)–O(8)	1.967(4)
Zn(1)–O(6)	1.948(4)	Zn(1)–O(10)	2.005(4)
2			
Cd(1)–O(10)	2.281(4)	Cd(2)–O(16)	2.216(4)
Cd(1)–O(8)	2.306(4)	Cd(2)–O(14)	2.266(4)
Cd(1)–O(6)	2.350(4)	Cd(2)–O(19)	2.313(4)
Cd(1)–O(5)	2.362(4)	Cd(2)–O(20)	2.345(4)
Cd(1)–O(4)	2.408(4)	Cd(2)–O(18)	2.437(4)
Cd(1)–O(7)	2.414(4)	Cd(2)–O(17)	2.553(4)
Cd(1)–O(9)	2.488(4)	Cd(2)–O(15)	2.577(4)

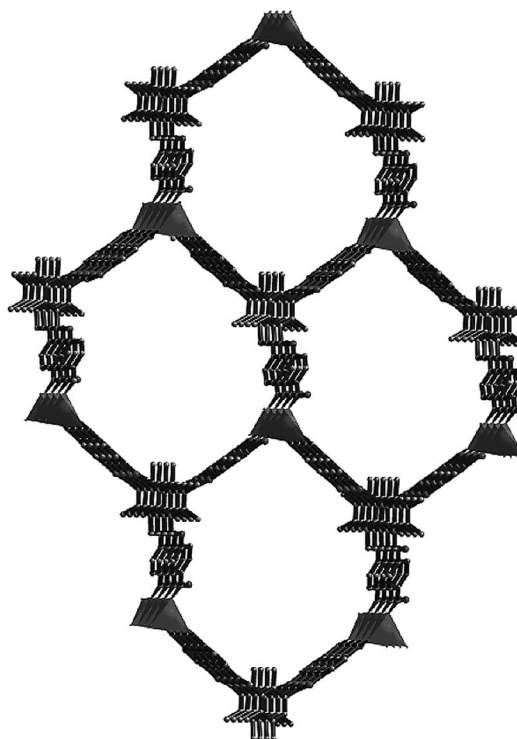


Figure 1. A view of a 3D network in complex **1** with hexagonal channels (helices) viewed down crystallographic *b* axis.

carboxylate groups is protonated at O9 as the C–O bond (C33–O9) is longer than the C33–O8 bond length. Because of the flexibility, the three different donor sites of the ligand are not in the same plane (oriented towards crystallographic *b* axis) and hence generate a 3D network with helical channels along the same direction (Figure 1). TOPOS^[22] analysis indicates

that the framework has uninodal 6-connected plane nets with point symbol of $(3^3.5^9.6^2.7)$ and sda topology.^[23]

An interesting structural feature of the complex is that the two 3D helical nets with opposite handedness are mutually entwined and extended along the crystallographic *b* axis with same helix pitch of 8.394(4) Å. Thus, the overall structure of the complex is a pair of enantiomers, leading to the racemization of the whole framework (Figure 2 and Figure 3). The solvent accessible volume of the complex **1** in each unit cell is 5207.0 Å³, which is 50.8% of the total volume of the unit cell (10242.0 Å³), and occupied by severely disordered solvent molecules (DMF and water).

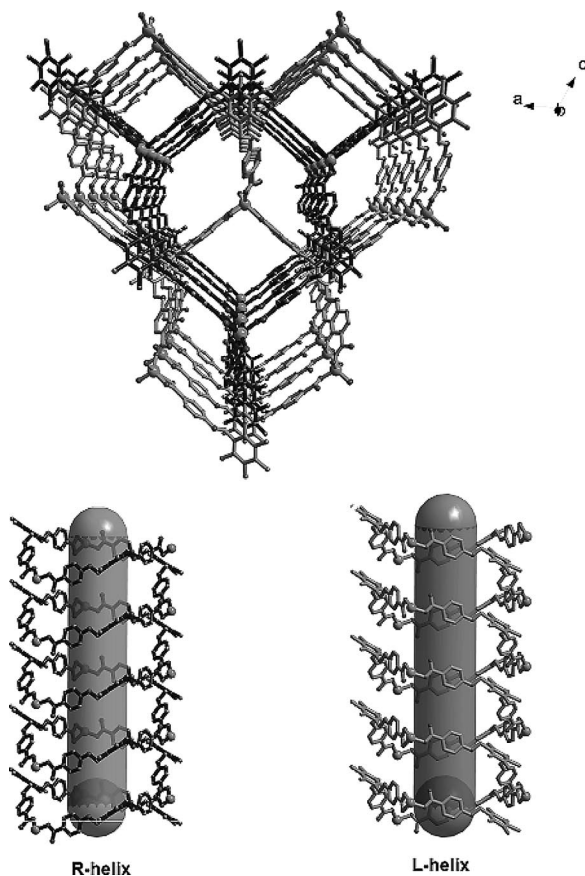


Figure 2. Two-fold interpenetrated 3D helical networks of **1** where nets with right and left handedness are shown.

Crystal Structure of $\{[(\text{CH}_3)_2\text{NH}_2]_2[\text{Cd}_2\text{L}_2(\text{DMA})_2]\}_n$ (**2**)

Single crystal structure analysis reveals that complex **2** is an anionic 2D layer framework that crystallizes in the triclinic centrosymmetric space group $P\bar{1}$. The asymmetric unit consists of two different molecular units (A and B; Figure S4, Supporting Information) with slight differences in their bonding parameters. Each unit consists of one seven-coordinate Cd^{II} ion, one L³⁻ ligand, one coordinated DMA molecule, and one $[(\text{CH}_3)_2\text{NH}_2]^+$ cation, which stays outside the metal coordination sphere (Figure S4). It must be pointed out that the amide solvent (DMA) not only serves as reaction medium but also

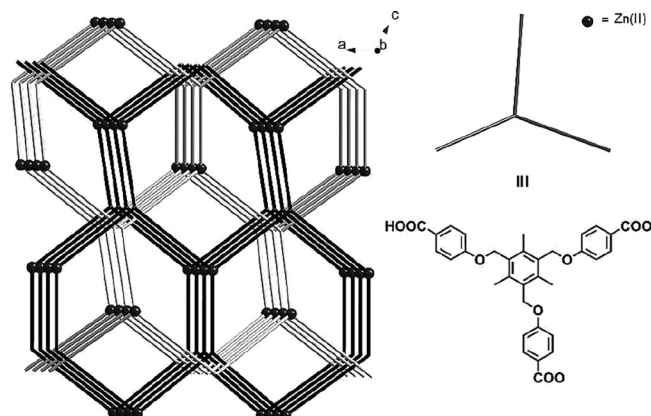


Figure 3. Schematic representation of the twofold interpenetration in **1**.

decomposes to provide charge-balancing cations, which eventually stabilize the anionic framework.

The coordination environment of Cd^{II} ions is completed by six oxygen atoms from three different carboxylate groups of three distinct L³⁻ ligands and one oxygen atom of the coordinated DMA molecule. Thus, each Cd^{II} ion is connected to three L³⁻ ligands in η^2 mode of coordination, and each L³⁻ is connected to three Cd^{II} ions, resulting in 2D sheets or nets. The structures of the 2D sheets are similar to previously reported $[\text{Cd}_2(\text{HBTB})_2(\text{DMF})(\text{MeOH})]$ (BTB = benzene-1,3,5-tribenzoate).^[24] The 2D sheets are interconnected by hydrogen bonds formed between carboxylate groups and $[(\text{CH}_3)_2\text{NH}_2]^+$ cations present in the lattice cavities (Table 2). Due to the large aperture of the hexagonal cavities in these sheets, a fourfold interpenetration results as shown in Figure 4 (top), where the individual sheets are held together by strong N–H \cdots O bonding formed between carboxylate groups and $[(\text{CH}_3)_2\text{NH}_2]^+$ cations. A view down the *b* axis reveals that several such interwoven 2D nets are stacked one over other through N–H \cdots O interactions between them, to result in a final layered structure (Figure 4 bottom and Figure 5).

Table 2. Hydrogen bond parameters (distances in Å and angles in °) of **2**.

D–H \cdots A	<i>d</i> (D–H)	<i>d</i> (H \cdots A)	<i>d</i> (D \cdots A)	\angle (DHA)
N(3)–H(3D) \cdots O(17)#1	0.90	2.09	2.830(8)	138.6
N(3)–H(3D) \cdots O(15)#1	0.90	2.45	3.117(10)	131.5
N(3)–H(3C) \cdots O(4)#2	0.90	2.63	3.107(8)	114.4
N(4)–H(4D) \cdots O(6)#3	0.90	1.89	2.771(6)	166.2
N(4)–H(4C) \cdots O(5)#4	0.90	1.94	2.827(7)	166.5

Symmetry transformations used to generate equivalent atoms: #1 $-x + 1, -y + 1, -z + 1$ #2 x, y, z #3 $x, y, z + 1$ #4 $-x + 2, -y + 1, -z + 1$.

The two-dimensional sheets feature uninodal 6-connected plane nets with point symbol of $(3^6.4^6.5^3)$ as revealed by TOPOS^[22] analysis. The solvent accessible volume of the complex **2** is 1096.6 Å³, which is 24% of the total volume (4569.0 Å³) and occupied by solvent molecules (DMA and water). The Cd–O bond lengths range from 2.224(4)–2.554(4) Å (Table 1).

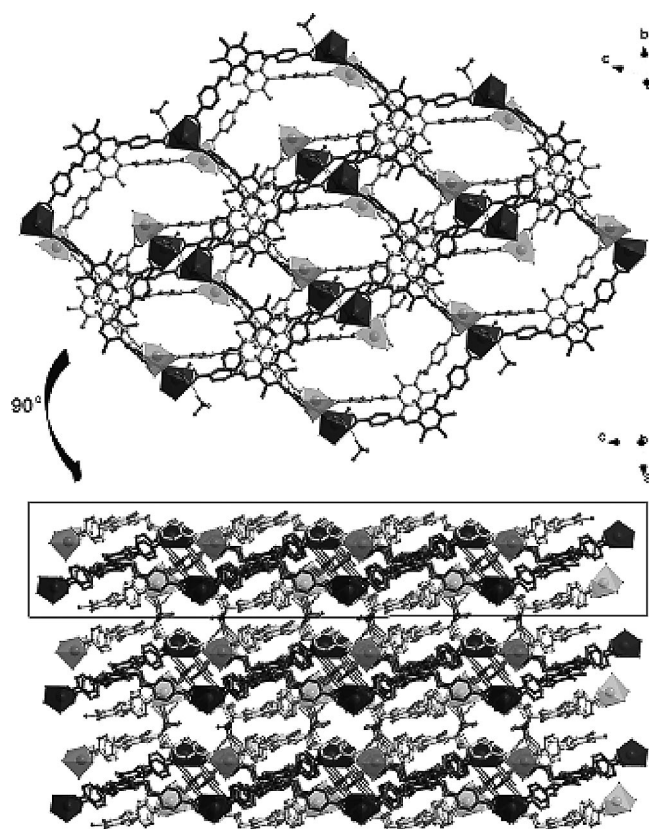


Figure 4. Crystal structure of **2**, layered structure (top) and a section of one of the layers of **2**, where four 2D nets are interwoven.

Conclusions

We have reported two new MOFs of Zn^{II} and Cd^{II} , which utilize a bent and flexible tri-carboxylic acid ligand. The complexes were characterized by elemental analysis, FT-IR spectroscopy, thermogravimetry, and single crystal XRD. The studies reveal that the diversity in metal coordination number and ligand flexibility play a significant role in producing helical architectures. The X-ray structure analyses reveal that Zn^{II} exhibits tetrahedral arrangement and culminates in a 3D helical structure, whereas the seven coordinate Cd^{II} ions afford a 2D layered framework made of interwoven nets. The large solvent accessible pores suggest the possibility of de-solvation and subsequent use of these materials for gas adsorption studies. We are investigating these possibilities along with efforts to isolate new MOFs with other transition metals employing H_3L as a prototype flexible ligand.

Experimental Section

Methods, Materials, and Instruments: All the starting materials and the products were found to be stable towards moisture and air, and hence no specific precaution was taken while handling them. Starting materials such as $\text{Zn}(\text{NO}_3)_2 \cdot 6\text{H}_2\text{O}$, $\text{Cd}(\text{NO}_3)_2 \cdot 4\text{H}_2\text{O}$, *N,N*-dimethylacetamide (DMA) and *N,N*-dimethylformamide (DMF) were procured from Merck, India.

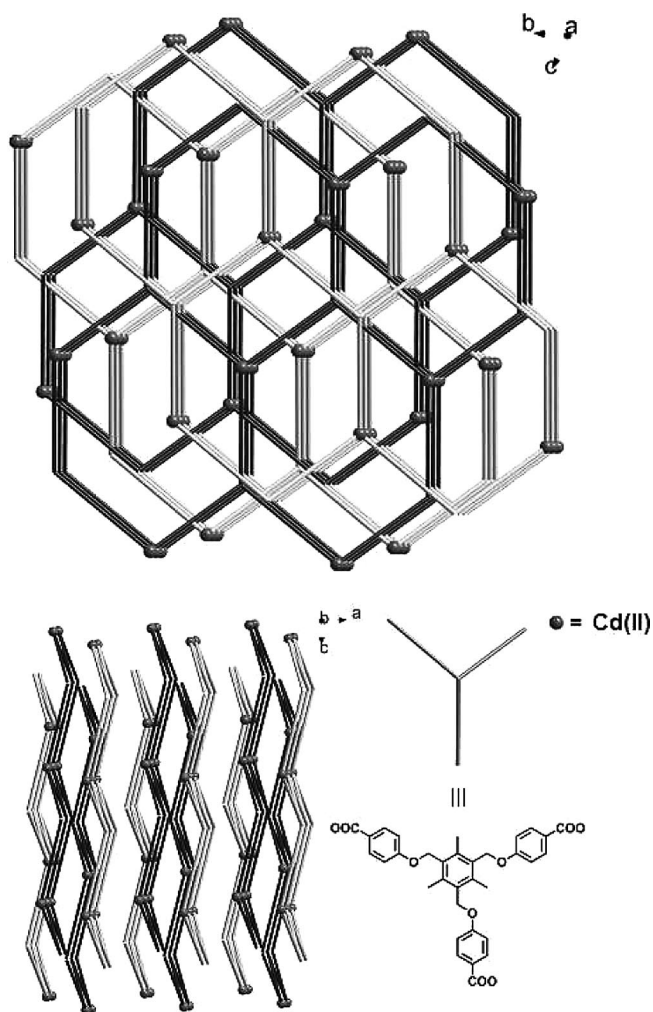


Figure 5. Schematic representation of the fourfold interwoven 2D nets in **2**.

Elemental analyses were performed with a Thermo Finnigan (FLASH EA 1112) microanalyzer. FT-IR spectra were recorded with a Perkin-Elmer Spectrum One Infrared Spectrometer as KBr diluted disks. Thermogravimetric analyses were performed with a Perkin-Elmer Pyris Diamond TGA instrument. Single crystal X-ray diffraction measurements were performed using Mo-K_α radiation ($\lambda = 0.71075 \text{ \AA}$) with a Rigaku AFC10K Satrun 724HG based diffractometer. PXRD data were collected with a Rigaku SmartLab X-ray diffractometer equipped with Cu-K_α radiation ($\lambda = 1.54056 \text{ \AA}$). Nitrogen adsorption / desorption experiments were performed isothermally at 77 K on Quantachrome autosorb-1.

Synthesis of H_3L : A mixture of methyl-*p*-hydroxybenzoate (7.6 g, 50.0 mmol), NaOH (4.0 g, 100 mmol) and DMSO (100 mL) was stirred at 75 °C for 1 h. To this hot mixture, 1,3,5-tris(bromomethyl)-2,4,6-trimethylbenzene (5.98 g, 15.0 mmol) was added and the resulting mixture was heated for another 24 h at 75 °C. The mixture was cooled to room temperature and poured into 200 mL of distilled water. To this, 50 mL aqueous solution of NaOH (20.0 g, 250 mmol) was added and heated for another 12 h at 75 °C. The mixture was again cooled to room temperature and acidified with diluted HCl (final pH ca. 2). A white precipitate formed immediately upon acidification was filtered under suction and washed repeatedly with water and with di-

ethyl ether and dried under vacuum to obtain analytically pure acid H₃L as white powder. Yield; 5.65 g, 73%. Mp 270–275 °C. C₃₃H₃₀O₉: C 69.46; H 5.30%; found: C, 69.34; H, 5.37%. ¹H NMR (400 MHz, [D₆]DMSO, 295 K): δ = 12.69 (s, 3 H, COOH), 7.93 (d, ³J_{HH} = 8.72 Hz, 6 H, ArH), 7.17 (d, ³J_{HH} = 7.76 Hz, 6 H, ArH), 5.21 (s, 6 H, BzCH₂), 2.36 (s, 9 H, ArCH₃) ppm. ¹³C{¹H} NMR (100 MHz, [D₆]DMSO, 295 K): δ = 167.0, 162.4, 139.2, 131.4, 131.2, 123.3, 114.5, 65.1, 15.6 ppm. LR-MS (ESI); m/z calcd. for C₃₃H₃₁O₉⁺ 571.19, found 571.14 [M + H]⁺. FT-IR (KBr): ν̄ = 3400–2600, 1682, 1603, 1510, 1428, 1244, 1168 cm⁻¹.

Synthesis of [Zn(HL)(H₂O)]_n (1): A mixture of H₃L (0.057 g 0.10 mmol), Zn(NO₃)₂·6H₂O (0.060 g 0.20 mmol), DMF (4.0 g), and distilled H₂O (1.0 g) was placed in a 20 mL glass vial and stirred for half an hour. The mixture was transferred to a 15 mL Teflon vial. The Teflon vial was placed inside a stainless steel autoclave and heated at 115 °C for 5 d. Microcrystalline solid was obtained upon cooling the reaction mixture to room temperature at the ambient conditions. The mixture was filtered and the filtrate was kept at room temperature to obtain needle like colorless crystals of **1** after a month. Yield; 0.04 g (61% based on H₃L used). Mp; > 250 °C. C₃₃H₃₀ZnO₁₀: C 60.8; H 4.6%; found: C 57.2; H 4.6%.^[25] FT-IR (KBr): ν̄ = 3433, 2925, 1604, 1385, 1223 cm⁻¹.

Synthesis of [(CH₃)₂NH₂]₂[Cd₂L₂(DMA)₂]_n (2): A mixture of H₃L (0.057 g, 0.10 mmol), Cd(NO₃)₂·4H₂O (0.062 g, 0.2 mmol), DMA (5.0 g), and distilled H₂O (1.0 g) was placed in a 20 mL glass vial, stirred for half an hour, and transferred to a 15 mL Teflon vial. The Teflon vial was placed inside a stainless steel autoclave and heated at 115 °C for 5 d. Colorless crystals of **2** were obtained after cooling the mixture to room temperature over 2 d. Yield; 0.06 g (74% based on H₃L used). Mp; > 250 °C. C₃₉H₄₄CdN₂O₁₀: C 57.6; H 5.4; N 3.4%; found: C 56.0; H 5.6; N 2.7%.^[25] FT-IR (KBr): ν̄ = 3389, 3073, 2957, 2921, 1604, 1542, 1385, 1239 cm⁻¹.

X-ray Crystallography: The single-crystal X-ray data were collected with a Rigaku Saturn 724 CCD diffractometer with a Mo-K_α radiation source (λ = 0.71075 Å) at 150 K under continuous flow of nitrogen. The data integration and indexing were performed using Rigaku Crystalclear software and a multi-scan method was employed to correct for absorption. The structures were solved by direct methods using SIR-92^[26] and refined by full-matrix least-squares fitting on F² using SHELXL-97.^[27] All the non-hydrogen atoms were refined anisotropically. The C–H protons were placed in their geometrical idealized positions and refined isotopically as riding atoms. The hydrogen atoms attached to oxygen were located in the difference Fourier maps and refined as rigid atoms in their idealized positions. Fourier maps also indicate severely disordered solvent molecules in the cavities. To account for the disordered solvent molecules, the final refinement was performed with modification of the structure factors using the SQUEEZE option of PLATON. Squeeze removed the solvent molecules from the voids which account for the difference in the elemental analyses. The solvent accessible volumes were calculated using CALC SOLV utility of PLATON. The data refinement details are given in Table 3

Crystallographic data (excluding structure factors) for the structures in this paper have been deposited with the Cambridge Crystallographic Data Centre, CCDC, 12 Union Road, Cambridge CB21EZ, UK. Copies of the data can be obtained free of charge on quoting the depository numbers CCDC-978029 for **1** and CCDC-978030 for **2** (Fax: +44-1223-336-033; E-Mail: deposit@ccdc.cam.ac.uk, http://www.ccdc.cam.ac.uk)

Table 3. Crystallographic data and structure refinement summary for complexes **1** and **2**.

	1	2
Formula	C ₃₃ H ₃₀ ZnO ₁₀	C ₃₉ H ₄₄ CdN ₂ O ₁₀
Formula wt	651.94	813.16
Temperature /K	150(2)	150(2)
Wavelength /Å	0.71075	0.71075
Crystal system	monoclinic	triclinic
Space group	C2/c	P1̄
a /Å	36.991(14)	14.275(5)
b /Å	8.394(3)	18.902(5)
c /Å	36.940(15)	19.667(7)
α /°	90	67.586(16)
β /°	116.750(5)	85.46(2)
γ /°	90	68.972(16)
Volume /Å ³	10242(7)	4569(3)
Z	8	4
Density (calcd) /g·cm ⁻³	0.846	1.182
Absorption coeff /mm ⁻¹	0.514	0.527
F(000)	2704	1680
Crystal size /mm ³	0.28 × 0.23 × 0.08	0.20 × 0.11 × 0.02
θ range /°	3.05 to 25.00	2.12 to 25.00
Reflection collected	34298	34619
Data (Rint)	8908 (0.0601)	15926 (0.0500)
Completeness to θ /%	99.9	99.0
Restraints/parameters	7/397	8/938
R ₁ [I > 2σ(I)] /all data	0.0920 / 0.1072	0.0656 / 0.0879
wR ₂ [I > 2σ(I)] /all data	0.2587 / 0.2725	0.1691 / 0.1838
Largest peak and hole /e·Å ⁻³	1.063, -0.874	0.494, -0.845

Supporting Information (see footnote on the first page of this article): FT-IR spectra, TGA profiles, metal coordination geometries, surface area measurement results, PXRD profiles, and the table containing selected bond distances and angles.

Acknowledgements

We sincerely thank SERB, DST, New Delhi for financial support for this work. We also thank the Department of Atomic Energy, Mumbai for a DAE-SRC Outstanding Investigator Award to RM, which made the purchase of a single crystal diffractometer possible. P. V. thanks CSIR, New Delhi for research fellowship.

References

- [1] K. Koh, A. G. Wong-Foy, A. J. Matzger, *J. Am. Chem. Soc.* **2009**, *131*, 4184–4185.
- [2] W. Morris, B. Voloskiy, S. Demir, F. Gándara, P. L. McGrier, H. Furukawa, D. Cascio, J. F. Stoddart, O. M. Yaghi, *Inorg. Chem.* **2012**, *51*, 6443–6445.
- [3] W. Chen, S. Fukuzumi, *Inorg. Chem.* **2009**, *48*, 3800–3807.
- [4] H.-L. Jiang, Y. Tatsu, Z.-H. Lu, Q. Xu, *J. Am. Chem. Soc.* **2010**, *132*, 5586–5587.
- [5] C. Wang, W. Lin, *J. Am. Chem. Soc.* **2011**, *133*, 4232–4235.
- [6] J. Lee, O. K. Farha, J. Roberts, K. A. Scheidt, S. T. Nguyen, J. T. Hupp, *Chem. Soc. Rev.* **2009**, *38*, 1450–1459.
- [7] W. Zhang, R.-G. Xiong, *Chem. Rev.* **2011**, *112*, 1163–1195.
- [8] R.-L. Sang, L. Xu, *Chem. Commun.* **2008**, 6143–6145.
- [9] a) Y.-K. Lv, C.-H. Zhan, Z.-G. Jiang, Y.-L. Feng, *Inorg. Chem. Commun.* **2010**, *13*, 440–444; b) B. Joarder, A. K. Chaudhari, S. K. Ghosh, *Inorg. Chem.* **2012**, *51*, 4644–4649.
- [10] E.-C. Yang, Z.-Y. Liu, X.-J. Shi, Q.-Q. Liang, X.-J. Zhao, *Inorg. Chem.* **2010**, *49*, 7969–7975.
- [11] E.-C. Yang, T.-Y. Liu, Q. Wang, X.-J. Zhao, *Inorg. Chem. Commun.* **2011**, *14*, 285–287.

- [12] Y. Bai, C.-y. Duan, P. Cai, D.-b. Dang, Q.-j. Meng, *Dalton Trans.* **2005**, 2678–2860.
- [13] Q. Sun, Y. Bai, G. He, C. Duan, Z. Lin, Q. Meng, *Chem. Commun.* **2006**, 2777–2779.
- [14] J. Ji, Y. Zhang, Y.-F. Yang, H. Xu, Y.-H. Wen, *Eur. J. Inorg. Chem.* **2013**, 2013, 4336–4344.
- [15] R. Murugavel, P. Kumar, M. G. Walawalkar, R. Mathialagan, *Inorg. Chem.* **2007**, 46, 6828–6830.
- [16] J. Y. Lu, V. Schauss, *Inorg. Chem. Commun.* **2003**, 6, 1332–1334.
- [17] S. Kitagawa, R. Kitaura, S.-i. Noro, *Angew. Chem. Int. Ed.* **2004**, 43, 2334–3773.
- [18] J.-Q. Chen, Y.-P. Cai, H.-C. Fang, Z.-Y. Zhou, X.-L. Zhan, G. Zhao, Z. Zhang, *Cryst. Growth Des.* **2009**, 9, 1605–1613.
- [19] W. M. Bloch, C. J. Doonan, C. J. Sumby, *CrystEngComm* **2013**, 15, 9663–9671.
- [20] C. Ma, Y. Wu, J. Zhang, Y. Xu, B. Tu, Y. Zhou, M. Fang, H.-K. Liu, *CrystEngComm* **2012**, 14, 5166–5169.
- [21] J. Zhang, Y.-S. Xue, H.-M. Wang, M. Fang, H.-B. Du, Y.-Z. Li, X.-Z. You, *Inorg. Chim. Acta* **2012**, 392, 148–153.
- [22] V. A. Blatov, A. P. Shevchenko, *TOPOS Version 4.0 Professional (beta evaluation)*, see: <http://www.topos.ssu.samara.ru>.
- [23] V. A. Blatov, D. M. Proserpio, in *Modern Methods of Crystal Structure Prediction*; Wiley-VCH Verlag GmbH & Co. **2010**, pp 01–28.
- [24] K. P. Rao, M. Higuchi, J. Duan, S. Kitagawa, *Cryst. Growth Des.* **2013**, 13, 981–985.
- [25] The accuracy of the elemental analysis is affected by the presence of solvent molecules in the pores of the framework.
- [26] G. Altomare, C. Giacovazzo, A. Guagliardi, *J. Appl. Crystallogr.* **1993**, 26, 343–350.
- [27] G. M. Sheldrick, *Acta Crystallogr., Sect. A* **2008**, 64, 112–122.

Received: December 23, 2013
Published Online: March 13, 2014